

## Combining Multiple Optimized FPGA-based Pulsar Search Modules Using OpenCL

Haomiao Wang, Prabu Thiagaraj, and Oliver Sinnen

Field-Programmable Gate Arrays (FPGAs) are widely used in the central signal processing design of the Square Kilometre Array (SKA) as acceleration hardware. The frequency domain acceleration search (FDAS) module is an important part of the SKA1-MID pulsar search engine. To develop for a yet to be finalised hardware, for cross-discipline interoperability and to achieve fast prototyping, OpenCL as a high-level FPGA synthesis approach is employed to create the sub-modules of FDAS. The FT convolution and the harmonic-summing plus some other minor sub-modules are elements in the FDAS module that have been well-optimised separately before. In this paper, we explore the design space of combining well-optimised designs, dealing with the ensuing need to trade-off and compromise. Pipeline computing is employed to handle multiple input arrays at high speed. The hardware target is to employ multiple high-end FPGAs to process the combined FDAS module. The results show interesting consequences, where the best individual solutions are not necessarily the best solutions for the speed of a pipeline where FPGA resources and memory bandwidth need to be shared. By proposing multiple buffering techniques to the pipeline, the combined FDAS module can achieve up to 2x speedup over implementations without pipeline computing. We perform an extensive experimental evaluation on multiple FPGA boards (Arria 10) hosted in a workstation and compare to a technology comparable mid-range GPU.

*Keywords:* pulsar search, frequency domain acceleration search, FPGA, OpenCL

### 1. Introduction

For a large scale global project such as the Square Kilometre Array (SKA)<sup>a</sup>, hundreds of research institutes and companies from over ten member countries are enrolled (Dewdney *et al.*, 2009). Each research group is assigned a small task such as one or several modules of the overall pipeline. After each module is investigated and optimised, it needs to be integrated with modules from other groups to form the whole pipeline. For software designs, different institutes can use the same operating system such as Linux and development environment. A large number of programming languages can be applied, and the software developers only need to make sure the external application programming interface (API) can be used by other groups.

Field-programmable gate arrays (FPGAs) and Graphics processing units (GPUs) are two main types of accelerators in radio astronomy projects. For GPU development, CUDA and OpenCL can be employed in the development and the details vary based on the GPU brand. In terms of FPGA development, the traditional synthesis flow needs hardware description languages (HDLs) such as Verilog HDL and VHDL, which is hard to understand let alone modify for SKA collaborators (e.g., software engineers and physicists) without expert knowledge in hardware design. Besides the traditional flow, a large number of high-level synthesis tools support a variety of high-level languages (compared to HDLs) such as OpenCL (Czajkowski *et al.*, 2012), C/C++, and Java (Costabile, 2011). In the SKA project, a framework that executes across heterogeneous platforms such as OpenCL is an excellent option for prototyping designs using acceleration hardware. By applying OpenCL, the same kernel codes can be executed on both FPGAs and GPUs without substantial modification, providing the same functionality of the design. While this is very useful, the performance of a single OpenCL design might vary strongly across platforms, due to the difference between the structures of FPGAs and GPUs, and require some 'performance porting' between different types of devices. The use of OpenCL makes the code more accessible to non-hardware-designers, provides functional portability and easy generational upgrades within a device type.

---

<sup>2</sup>Corresponding author.

<sup>a</sup>[www.skatelescope.org](http://www.skatelescope.org)

In this research, we investigate the Fourier domain acceleration search (FDAS) module (Ransom, 2001) of the pulsar search engine (PSS) within the SKA1-MID central signal processor (CSP). The main function of the FDAS module is to remove the smeared pulsar signals by using the correlation technique (Ransom *et al.*, 2002; Jouteux *et al.*, 2002). It consists of two main parts: FT convolution sub-module and harmonic-summing sub-module. The FT convolution module is a compute-intensive application that contains 85 FIR filters, with up to 400 coefficients (or taps). The harmonic-summing module is a data-intensive application, and the main problem is the large number of irregular memory accesses during processing. These two modules have been individually investigated and well-optimised on high-end FPGAs using OpenCL in previous research. The optimised designs can gain better performance and consume less energy on FPGAs than that of GPU designs while meeting the requirements. However, the optimised performance might not be achieved when combining with other modules. More interestingly, optimisation choices might be different when sub-modules are part of a larger pipeline. We investigate in this paper the combination of well-optimised designs, explore the design space and optimise the combination of designs. The main contributions of this research are as follows:

- Design Space: explore the design space of combining investigated implementations; three types of data transformation methods are investigated to combine proposed FT convolution and harmonic summing implementations;
- Pipeline structure: adopting multiple buffering (double and triple buffering in this research) to improve the performance of investigated combinations;
- Multiple Devices: multiple acceleration devices are employed in processing the combined implementations. Different methods of partitioning the workload across devices are investigated.

The rest of the paper is organized as follows. Section 2 provides the details of straight-forward and optimised designs of the FT convolution module and the harmonic-summing module and states the design goals of the FDAS module. In Section 3, the design space of combining optimised modules is explored, and the pipeline structure is investigated on multiple devices. Section 4 presents the experimental evaluation results and their analysis. Finally, the conclusions are given in Section 5.

## 2. Frequency Domain Acceleration Search

The FDAS module illustrated in Figure 1 is a part of the SKA1-MID CSP element, and the required parameters are listed in Table 1. From the antennas, over 2,000 beams are formed at 4,096 frequency channels per beam. The signals of each beam are processed independently, and each beam needs a dedicated pulsar search engine. Because the dispersion measure, to compensate for signal changes due to travel through interstellar space, is unknown, over 6,000 trial values are tested, and several pulsar search approaches are employed such as time domain acceleration search and frequency domain acceleration search. The FDAS module consists of two main parts: 1) the FT convolution module and 2) the harmonic-summing module. Both these modules have been investigated and optimised for FPGAs before (the FT convolution module in (Wang *et al.*, 2016, 2018) and the Harmonic-summing module in (Wang *et al.*, 2018)), and we very briefly review the details in this section.

In previous research, different types of acceleration devices were employed to evaluate the performance of the straight-forward and optimised approaches. Two types of Intel high-end FPGAs (Stratix V, referred to as **S5**, and Arria 10, referred to as **A10**) are compared with one mid-range AMD R7 GPU, referred to as **R7**. The platform specifications are given in Table 2. The FPGA and GPU cards are connected to the host through the PCIe bus, and the structure of FPGA-based platform is depicted in Figure 2. For the FPGA acceleration cards, each one is connected through 8x lane PCIe bus (*S5* use PCIe Gen2.0 and *A10* use PCIe Gen3.0). Regarding the *R7* GPU board, it uses a 16x lane PCIe bus of Gen3.0. Gen3.0.

Apart from these PCIe card-based platforms, the Intel Xeon Scalable processor with an in-package Arria FPGA from the Hardware Accelerator Research Program (HARP) is employed in this research. The platform, referred to as *HARP*, has a 14 core Xeon processor at 2.4GHz and an Intel Arria 10 GX1150 FPGA, which is the same as the one on the *A10* card.

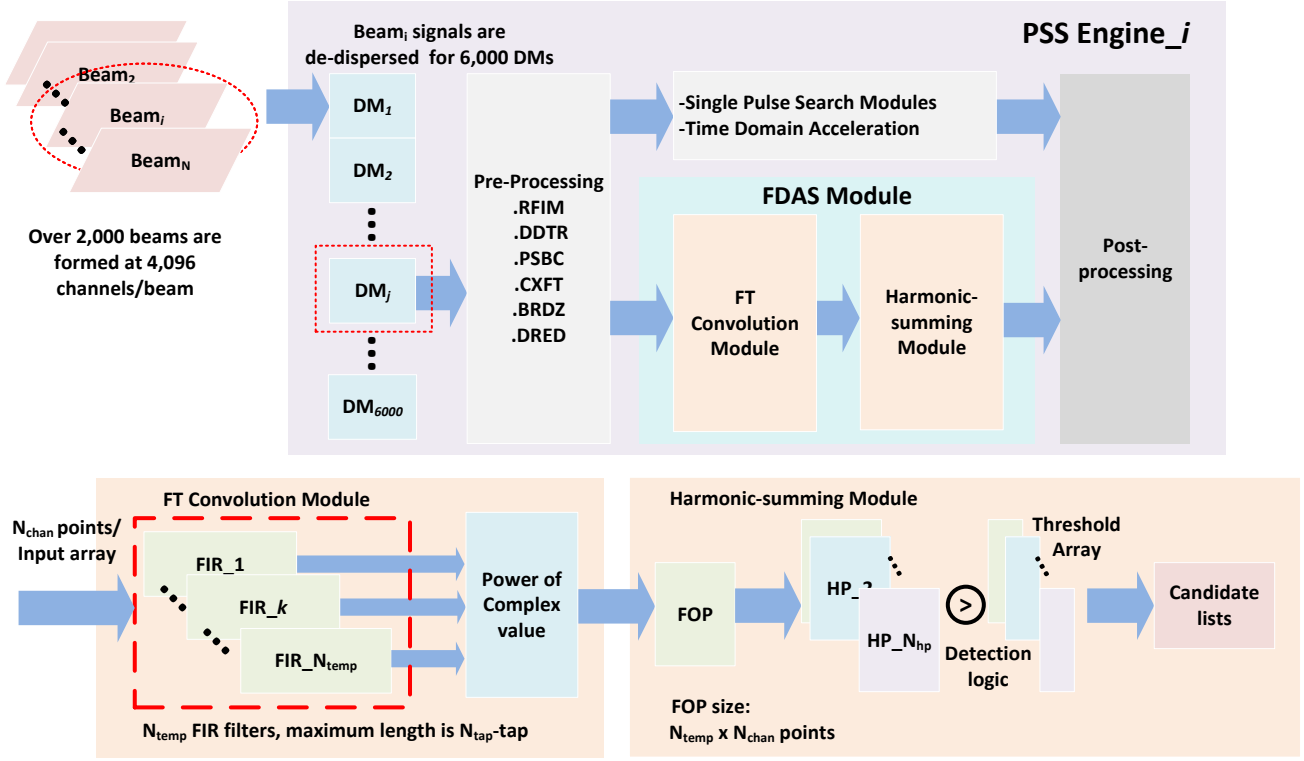


Figure 1. Processing flow of Pulsar Search Engine (PSS) of SKA1 CSP system and details of FDAS module

Table 1. FDAS Module Parameters

Parameter	Description	Value
$N_{beams}$	Number of beams	1000~2000
$N_{DM-trail}$	Number of de-dispersion measure (DM) trails	6000
$T_{obs}$	time period of each observation	540s
$N_{temp}$	Number of templates (row of the FOP )	85
$N_{chan}$	Number of channels (column of the FOP)	$2^{21}$
$N_{tap}$	Number of FIR filter taps for each template	421
$N_{hp}$	Total number of harmonic planes	8
$N_{cand}$	Number of candidates per harmonic plane	200

### 2.1. FT Convolution Module

The core computation part of the FT convolution module is to process  $N_{chan}$  points with  $N_{temp}$  FIR filters. The basic FIR filter implementation is investigated in both time domain (TDFIR) and frequency domain (FDFIR).

#### Frequency domain – FDFIR

Naïve TDFIR

The TDFIR filter is a straight-forward implementation of equation 1

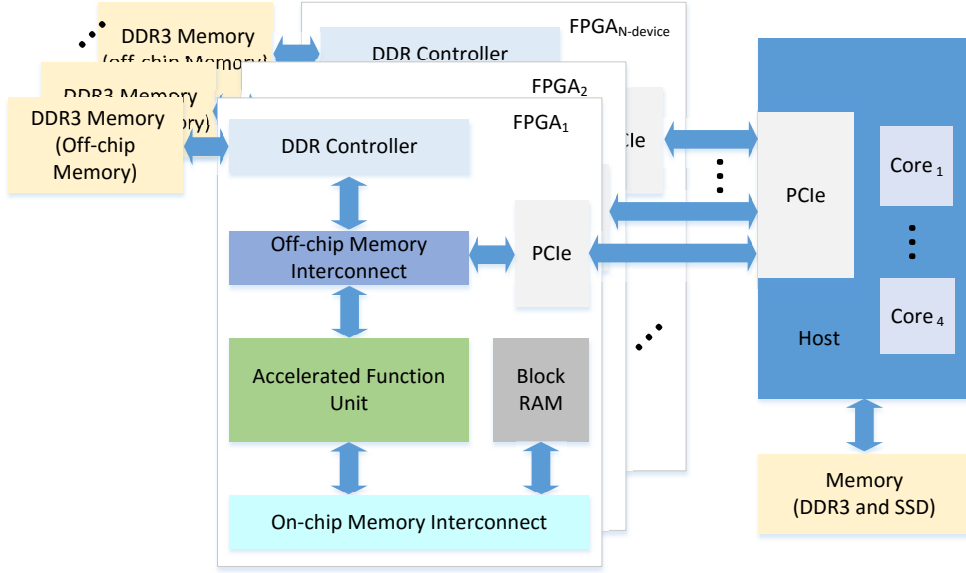


Figure 2. Structure of the high-end FPGA devices as acceleration hardware in a host system

Table 2. Details of CPU, GPU and FPGA Platforms

Device	Terasic DE5-Net (S5)	Nallatech 385A (A10)	Sapphire Nitro R7 370 (R7)	Intel CPU Host (I7)
Hardware	Intel Stratix V 5SGXA7	Intel Arria 10 GX1150	AMD Radeon R7 370	Intel Core i7-6700K
Technology	28nm	20nm	28nm	14nm
Compute resource	622,000 LEs	1,506,000 LEs	1,024 Stream Processors	8 Processors
On-chip memory size	256 DSP blocks	1,518 DSP blocks	(16 Compute Units)	(4 Cores)
Off-chip memory size	50Mb	53Mb	—	64Mb
Memory interface width	2 x 2GB DDR3	2 x 4GB DDR3	4GB GDDR5	64GB DDR4
Max clock frequency	2 x 64-bit	2 x 72-bit	256-bit	—
Max power consumption	600MHz	1.5GHz	985MHz	4.2GHz
	—	75W	150W	—

$$y[i] = \sum_{j=0}^{N_{tap}-1} x[i-j]h[j], \text{ for } i = 0, 1, \dots, N_{chan} - 1, \quad (1)$$

where  $x[\cdot]$ ,  $h[\cdot]$ , and  $y[\cdot]$  are complex single precision input signals, coefficients, and output results, respectively.

#### Overlap-add Algorithm based TDFIR

The amount of logic resources and DSP blocks in a specific FPGA are fixed. If the FIR filter size  $N_{tap}$  is too large, an FPGA does not have enough logic resources and DSP blocks to parallelise  $N_{tap}$  complex multiplications and then fails to achieve a pipeline structure. To make an  $N_{tap}$ -tap FIR filter fit into the targeted FPGA and maintain high-performance, we apply the overlap-add algorithm (**OLA**) to split the coefficient array into a group of sub-arrays (Pavel & David, 2013).

## Frequency domain – FDFIR

### Naïve FDFIR

Based on the convolution theorem, Equation (2), the output of an FIR filter can be obtained by the following three steps (Steven *et al.*, 1997): 1) Fourier transform of the input array and coefficient array, 2) element-wise multiplication of these two arrays, and 3) inverse Fourier transform of the output array.

$$x * h = \mathcal{F}^{-1}\{\mathcal{F}\{x\} \cdot \mathcal{F}\{h\}\}, \quad (2)$$

where  $\mathcal{F}\{\cdot\}$  and  $\mathcal{F}^{-1}\{\cdot\}$  are Fourier transform and inverse Fourier transform.

### Overlap-save Algorithm based FDFIR

For large input size Fourier transforms, such as the targeted two million points ( $2^{21}$ ) FFT, the on-chip memory of an FPGA is unable to store all points, which makes it impossible to perform the complete process as described in Equation (2) in one go. Hence, we apply the overlap-save algorithm (OLS) to split the input signals into chunks (Pavel & David, 2013). Each chunk overlaps with its two neighbour chunks, and the extent of the overlap is  $N_{tap} - 1$ . For the first input chunk,  $N_{tap} - 1$  zero points have to be padded at the beginning. After convolving in frequency-domain, the overlap, which is the first  $N_{tap} - 1$  points of each chunk, are discarded.

### Optimised Performance

The straight-forward and optimised implementations of a single FIR filter are evaluated, and the execution latencies of these kernels are given in Figure 3. For TDFIR kernels, the value 64 represents a completely parallelised 64-tap FIR filter. The *S5* FPGA has 256 DSP blocks and 64 complex SPF multiplications are the largest scale it can parallelise. **AOLS** is the area-efficient OLS-FDFIR that contains only one FFT engine (radix-4 feed-forward FFT (Garrido *et al.*, 2013)). The AOLS kernels have to be launched twice to process one input array. The **TOLS** is the time-efficient OLS-FDFIR that contains two FFT engines. The number after AOLS and TOLS in the legend of Figure 3 indicates the size of the point chunks.

The experiments in (Wang *et al.*, 2016) demonstrated that TOLS-1024 is the fastest among these kernels in implementing *one* FIR filter. For  $N_{temp}$  FIR filters, kernel TOLS-1024 has to Fourier transform the same input array  $N_{temp}$  times. The AOLS kernels then become efficient since it can Fourier transform the input array once and then launch  $N_{temp}$  times to implement  $N_{temp}$  FIR filters.

Using the fastest implementation of the optimised designs (AOLS-2048), the pipeline is slightly extended to include the power calculation of the complex filter outputs and then evaluated on two types of FPGA devices and one GPU device. The results over varying numbers of FIR filters are given in Figure 4. For FPGAs, the results are based on employing three cards, and the same AOLS-2048-P kernel can be replicated 3x times on each *S5* and 4x times on each *A10*. It can be seen that three *A10* cards can execute the FT convolution module in about 50ms, and it is 1.3x times faster than the single *R7* GPU, which uses significantly more power than three FPGA boards.

## 2.2. Harmonic-summing Module

The FT convolution output is the Filter-Output-Plane (FOP) that is sent to the harmonic-summing module for candidate detection. In the harmonic-summing module, which is described in Algorithm 1, the FOP is stretched by a group of integers to generate  $N_{hp}$  stretch planes (*SPs*). The FOP and stretch planes are accumulated to calculate  $N_{hp}$  harmonic planes (*HPs*) and then threshold-detection logic is applied to collect  $N_{cand}$  candidates from each harmonic plane. All operations in the harmonic-summing module are inexpensive operations such as floating-point additions and comparisons with a constant. The FOP takes up to 710MBytes under current requirements, which is tens of times larger than the on-chip memory size of a high-end FPGA, so it has to be stored in the off-chip memory (i.e., DDR RAM on FPGA board) in the FT convolution module. The main issue for this module is the large number of irregular off-chip memory accesses, and we optimised this issue using two approaches: 1) reducing the number of accesses and 2) increasing the used off-chip memory bandwidth (Weinhardt & Luk, 1999).

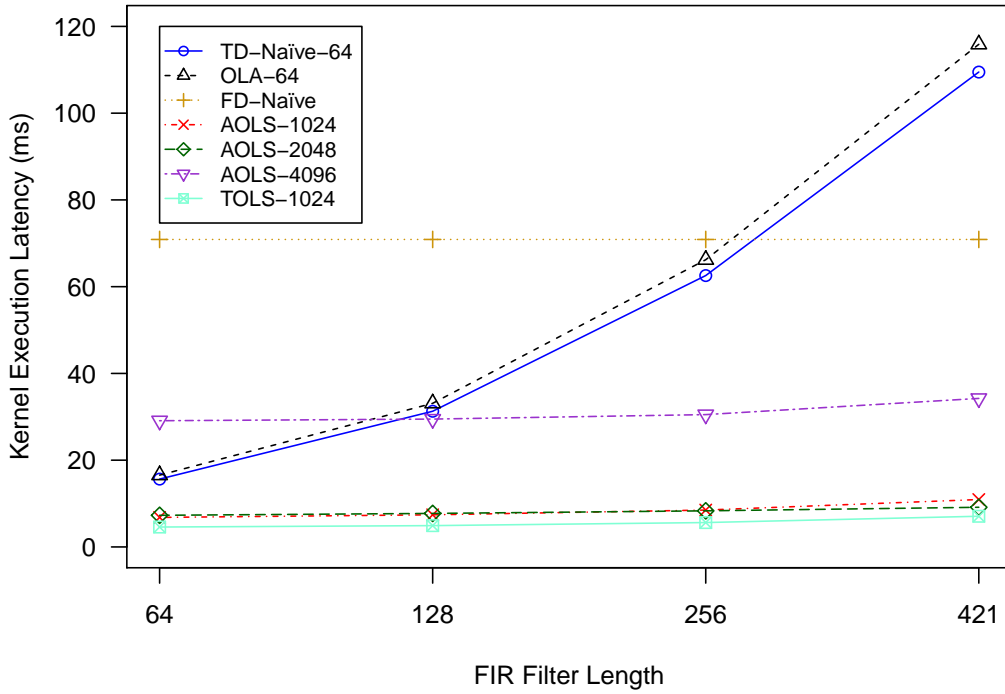


Figure 3. Execution latency of a single FIR filter using TDFIR and FDFIR based kernels on one S5

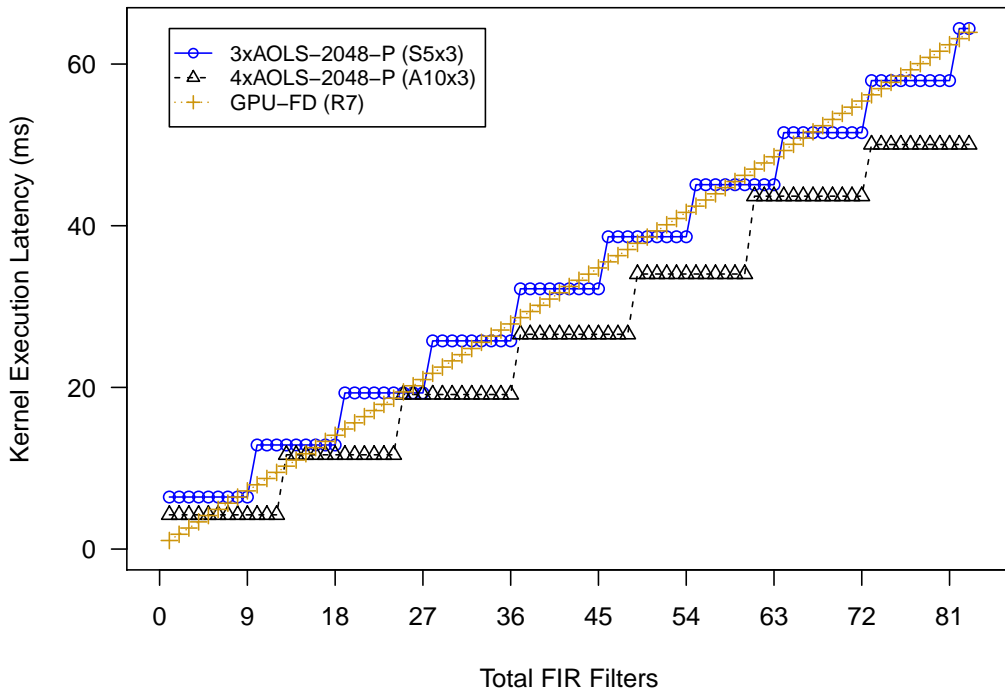


Figure 4. Execution latency of AOLS-2048 kernel using three S5 and A10 FPGAs, and a single R7 GPU

Two types of methods for the processing in the harmonic-summing module were investigated: SINGLEHP, where a single harmonic plane is processed at a time, and MULTIPLEHP, where multiple harmonic planes are processed simultaneously. The optimised methods are listed below and the parameters are described in Table 3.

---

**Algorithm 1** Harmonic-summing Algorithm
 

---

```

 $SP_1 \leftarrow$  (filter-output-plane (FOP))
 $CL \leftarrow 0$  {initialize the detection output}
for  $k = 1$  to  $N_{hp}$  do
  for  $i = -(N_{temp} - 1)/2$  to  $(N_{temp} - 1)/2$  do
    for  $j = 0$  to  $N_{chan} - 1$  do
       $SP_k(i, j) \leftarrow$  stretch( $SP_0, k, i, j$ ) {generate the value in stretched plane}
       $HP_k(i, j) \leftarrow HP_{k-1}(i, j) + SP_k(i, j)$  {based on the stretched plane, generate the value in harmonic plane}
       $CL \leftarrow$  detection[ $HP_k(i, j), TA(k, i)$ ] {threshold-detection logic to identify valid peak signals}
    end for
  end for
end for
Candidate List  $\leftarrow CL$ 

```

---

- SINGLEHP
  - (a) SINGLEHP-( $S/M, V/R, N_{paral}$ )
- MULTIPLEHP
  - (a) Naïve MULTIPLEHP
  - (b) MULTIPLEHP-H-( $N_{MultipleHP-H-preld}$ )
  - (c) MULTIPLEHP-N-( $N_{MultipleHP-N-col}$ )
  - (d) MULTIPLEHP-R-( $N_{MultipleHP-R-col}, N_{points/wi}$ )

Table 3. Parameters of harmonic-summing methods

Parameter	Description
$S/M, V/R$	$S/M$ represents single or multiple launch(es) and $V/R$ represents vectrize or replicate the kernel
$N_{paral}$	Value of the parallelization factor
$N_{MultipleHP-H-preld}$	preloaded data size of the MULTIPLEHP-H method
$N_{MultipleHP-N-col}$	Number of processed columns of all $N_{hp}$ harmonic planes per work-group using MULTIPLEHP-N
$N_{MultipleHP-R-col}$	Number of processed columns of all $N_{hp}$ harmonic planes per work-group using MULTIPLEHP-R
$N_{points/wi}$	Number of processed points of all $N_{hp}$ harmonic planes per work item

The SINGLEHP method is a straight-forward implementation of Algorithm 1. The main advantage of MULTIPLEHP over SINGLEHP is that it is unnecessary to store harmonic planes in the off-chip memory during processing. The MULTIPLEHP-H method is based on the Naïve-MULTIPLEHP method, and it preloads the  $N_{MultipleHP-H-preld}$  points with the highest touching frequency in the FOP. Another loading method is MULTIPLEHP-N that loads all necessary points in the FOP that are needed to calculate  $N_{MultipleHP-N-col}$  columns of all  $N_{hp}$  harmonic planes. Though these methods can reduce the off-chip memory accesses to some degree, the accesses to the off-chip memory are still irregular.

The MULTIPLEHP-R method is based on the MULTIPLEHP-N method, however, the FOP is reordered and padded to generate the rFOP before processing. In the rFOP, the necessary points in the FOP that are needed to calculate a block of points in all  $N_{hp}$  planes are stored in consecutive memory addresses. This makes some points in the original FOP have to be stored in several places in the rFOP, which leads to an increase in the rFOP size. After reordering, the points in the rFOP can be streamed to FPGA during processing. Besides  $N_{MultipleHP-R-col}$ , the parameter  $N_{points/wi}$  is an important factor for the MULTIPLEHP-R method, and it is restricted by the resources of the target FPGA.

These different approaches were implemented using Intel FPGA-based OpenCL. For each method, the parameters for the best performing implementation and the resource usage and kernel execution latencies, including the candidate detection part, are presented in Table 4 and Figure 5. The red dot line in Figure 5 is the required time limitation and the execution latencies are for processing half FOP. Kernel MULTIPLEHP-R performs better than the other kernels, however, additional processing has to be done to reorder the

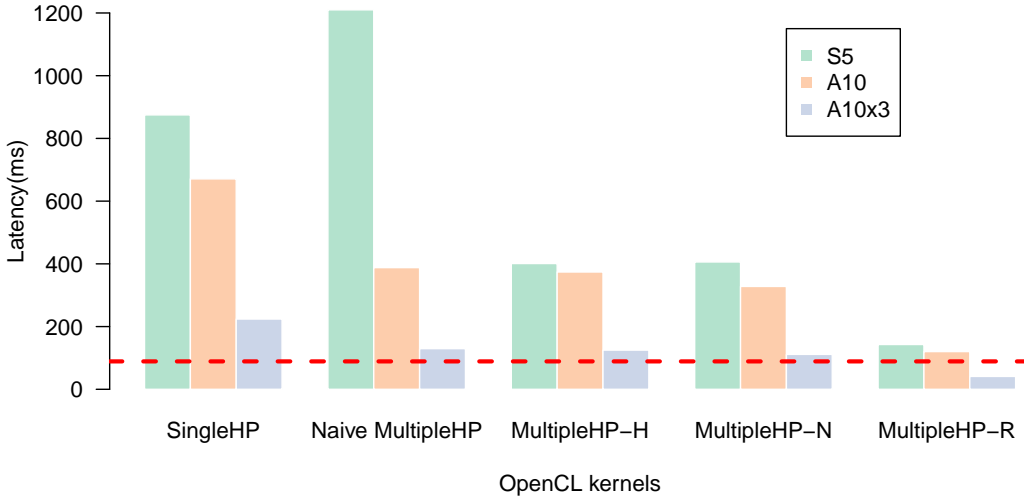


Figure 5. Execution latency of the straight-forward and optimised methods on two types of FPGA devices (x3 means three A10 FPGAs were used)

standard FOP. The reorder task can be done on both host and device. In the host program, the memory copy function `memcpy()` can handle this task efficiently. For the OpenCL kernel, there are no such functions and a block of points has to be copied to another place using a `for` loop. Although the host processor has the advantage over the FPGAs in reordering the FOP, the penalty for transferring data between host and device has to be considered.

Table 4. Resource usage and execution latency of the best harmonic-summing kernels on A10

Kernel-(Settings)	Logic utilization	RAM blocks	DSP Blocks	Kernel frequency (MHz)
SINGLEHP-( $S, R, 8$ )	42%	28%	<1%	206.1
Naïve MULTIPLEHP	17%	27%	<1%	227.06
MULTIPLEHP-H-( $5 \times 2^{13}$ )	19%	37%	<1%	235.84
MULTIPLEHP-N-(1)	17%	19%	<1%	276.54
MULTIPLEHP-R-(16, 4)	30%	37%	3%	196.88

Without including the candidate detection in the compilation and synthesis process, SINGLEHP-( $M, R, 16$ ) and MULTIPLEHP-R-(64, 8) can be successfully synthesized for the A10 FPGA, however including candidate detection (as done with the kernels in Figure 5) makes the synthesis fail due to exhausted FPGA resources. This is the same type of compromise we will see later when the modules are combined in the pipeline on the FPGA.

### 3. Combining Modules and Optimisation

#### 3.1. Design Goals

The FT convolution module and harmonic summing module are well-optimised, and each can meet the required time limitation using three high-end FPGAs. The goal of this research is to combine these two modules while meeting the requirements of the FDAS module, especially the time limitation.

As introduced above, the FDAS module contains two main parts: 1) FT convolution and 2) harmonic summing (including candidate detection). The accumulated latency of different parts is the overall latency  $t_{FDAS}$  of the FDAS module in processing one input array, namely the latencies of: the FT convolution (multiple FIR filters and power calculation)  $t_{FT}$ , the FOP preparation  $t_{FOP}$ , and the harmonic summing



$t_{HM}$ :

$$t_{FDAS} = t_{FT} + t_{FOP} + t_{HM}. \quad (3)$$

Latency  $t_{FT}$  is affected by three factors: the kernel launching overhead  $t_{klo}$ , the execution latency of each FT convolution kernel  $t'_{FT_i}$ , and the number of times  $N_{FT-launch}$  the kernel is launched. Hence,  $t_{FT}$  can be expressed as

$$t_{FT} = \sum_{i=1}^{N_{FT-launch}} t'_{FT_i} + \sum_{i=1}^{N_{FT-launch}} t_{klo_i}.$$

Depending on the combination of the FDAS sub-modules,  $t_{FOP}$  might consist of several parts such as discard  $t_{discard}$ , transpose  $t_{transpose}$ , and reorder  $t_{reorder}$  and can be expressed as

$$t_{FOP} = \mathbf{B}_1 t_{discard} + \mathbf{B}_2 t_{transpose} + \mathbf{B}_3 t_{reorder},$$

where the data types of  $\mathbf{B}_1$ ,  $\mathbf{B}_2$ , and  $\mathbf{B}_3$  are Boolean and the values depend on the combined sub-module kernels. Latency  $t_{HM}$  varies based on the applied method.

Regarding the FOP preparation, it is a module that is added between the FT convolution module and the harmonic-summing module, which is discussed in Section 3.2.

Based on the fastest results in Section 2.1 and Section 2.2, even the achievable  $t_{FDAS}$  is greater than  $t_{limit}$ . Because of the limited logic resources on the FPGA, the fastest implementations of two modules cannot be merged into one implementation. There are two alternatives: 1) keep the optimised kernels and 2) modify the optimised kernels to put the whole FDAS module in one FPGA device.

There are two options without modifying the optimised implementations: 1) use multiple FPGA devices or 2) reconfigure the FPGA device several times. For the first solution, the data transfer rate between the host and devices becomes an essential factor. With PCIe Gen3.0 for example, the theoretical latency of loading half FOP ( $42 \times 2^{21}$  points) from one device and sending it to another device is about the same as  $t_{limit}$ . If the FOP preparation module is assigned to the host processor, it makes the overall pulsar search pipeline impossible to meet the required time limit. Regarding the second solution, it takes over one second for both *S5* and *A10* to reconfigure the new bitstream file that is over 10x times larger than  $t_{limit}$  which leaves alternative 2. If the optimised kernels are modified to make all three modules fit into one FPGA device,  $t_{FDAS}$  becomes unimportant. The three parts of the FDAS module can work in parallel in a pipeline by employing multiple buffering. Taking the triple buffering as an example, each part can process points from different input arrays at the same time, and the slowest section of these three kernels determines the execution latency of a new input array. The combination of these three parts becomes an important issue. In this research, we investigate the suitable combination of the optimised implementations for a given FPGA device. The total number of combinations is the product of the number of FT convolution methods and the number of harmonic-summing methods. These combinations can be categorised into four types: TDFIR + SINGLEHP, TDFIR + MULTIPLEHP, FDFIR + SINGLEHP and FDFIR + MULTIPLEHP.

### 3.2. FOP Preparation

As introduced in Section 2.1 and 2.2, the output plane from the FT convolution and the needed plane for the harmonic summing varies based on different kernel approaches. To make the FT convolution output plane compatible with the harmonic summing input plane, the output from the FT convolution module has to be transformed, and we add an FOP preparation module to connect these two modules. There are three types of transform processing: (a) transpose, (b) discard, and (c) reorder, which are depicted in Figure 6.

For the TDFIR-based FT convolution kernels, each row of the output plane is the output from an FIR filter (Figure 6(a)). However, processing column by column might be more efficient for some harmonic summing kernels. In this case, the output plane has to be transposed.

The output plane of the FDFIR-based FT convolution kernels (Figure 6(b)) contains a number of slices of dummy/invalid points and these points need to be discarded to get the standard FOP.

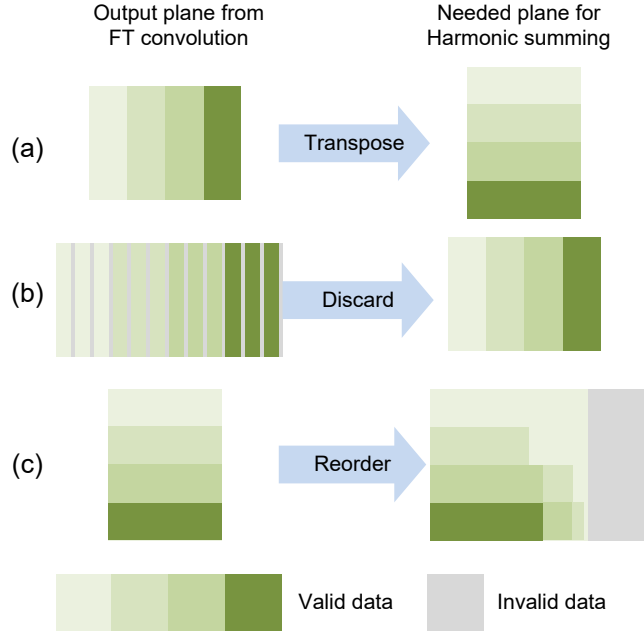


Figure 6. Three types of processing the output plane of the FT convolution module: (a) Transpose (b) Discard (c) Reorder.

The MULTIPLEHP-R kernel performs better than other MULTIPLEHP-based harmonic-summing kernels, however, the input plane is not the standard FOP but the reordered FOP (RFOP). To generate the RFOP, the output plane has to be padded and reordered (Figure 6(c)). The reason for padding with dummy data is to make the number of loaded points per clock cycle a power of two, which is more efficient than other numbers.

For different kernel combinations, these three types of transforms can be combined. If the output plane is the same as the needed input plane, the FOP preparation module can be removed. For example, if the FT convolution output plane is the left plane in Figure 6(b) and the needed input is the right plane in Figure 6(c), all these three transforms have to be applied in a certain order (discard + transpose + reorder) in the FOP preparation kernel.

### 3.3. Pipeline Computing

Instead of processing one input array, the FDAS module keeps running (24/7/365) when it is employed and will process a constant stream of input signals. The main purpose of this research is to optimise the execution latency of multiple input arrays, i.e. the throughput, but not the overall execution latency of a single input array  $t_{FDAS}$ . Therefore, we investigate the pipeline processing of the FDAS module. Given the three sub-modules, the ideal execution latency for each input array in a pipeline, which is the pipeline period, is  $\max(t_{FT}, t_{FOP}, t_{HM})$  and the number of required buffers depends on  $t_{FDAS}$  and  $\max(t_{FT}, t_{FOP}, t_{HM})$ , which is illustrated in Figure 7. If  $\max(t_{FT}, t_{FOP}, t_{HM}) \geq t_{FDAS}/2$ , double buffering can be employed, and when  $\max(t_{FT}, t_{FOP}, t_{HM}) < t_{FDAS}/2$ , it is recommended to adopt triple buffering.

Note that  $t_{FDAS}$  of the two combinations in Figure 7 are the same, but the  $\max(t_{FT}, t_{FOP}, t_{HM}) < t_{FDAS}/2$  combination performs better than the  $\max(t_{FT}, t_{FOP}, t_{HM}) \geq t_{FDAS}/2$  combination when employing pipeline processing, as the pipeline stages are more balanced in the latter case. For combinations where  $\max(t_{FT}, t_{FOP}, t_{HM}) \geq t_{FDAS}/2$ , the parallelisation factors of the three combined kernels can be adjusted to reduce  $\max(t_{FT}, t_{FOP}, t_{HM})$  to a value smaller than  $t_{FDAS}/2$  while aiming that  $t_{FDAS}$  is not increased. In other words, the objective of our research here is to minimise  $\max(t_{FT}, t_{FOP}, t_{HM})$  within the resource and bandwidth limits of the FPGA by carefully investigating how to best combine and configure the optimised kernels of the sub-modules.

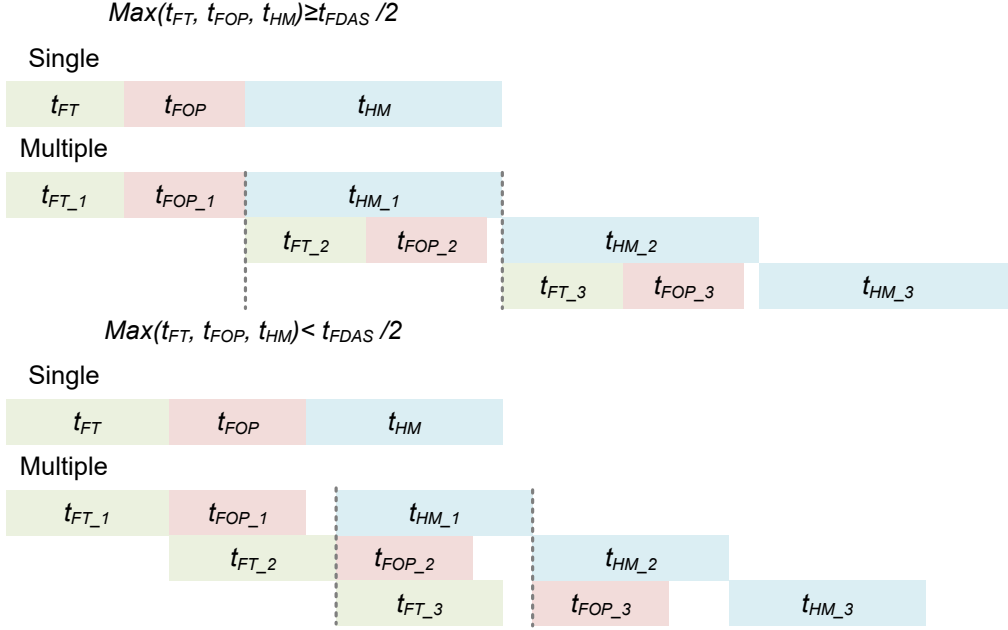


Figure 7. Execution latency of single and multiple input arrays using double and triple buffering

### Device Limitation

For most of the accelerators, the FPGA devices are connected to the host processor through the PCIe bus (Figure 2), which is introduced in Section 2. Three major parts can limit the device performance: FPGA resources, off-chip memory, and the data transfer bus.

### FPGA Resources

The logic cells, DSP blocks, and (embedded) RAM blocks are three main types of FPGA resources, and the limit of each kind of resource leads to different problems. The logic cells are employed to handle the necessary fixed-point operations and the shift register. The number of DSP blocks decides the number of parallelised floating-point operations such as multiplications. Regarding the RAM blocks, they are the main on-chip memory, and the number of RAM blocks restricts the amount of data that can be stored in local memory during processing.

### Off-chip Memory

Two factors regarding the off-chip memory are discussed: 1) data transfer rate and 2) off-chip memory size.

Because the FOP is stored in off-chip memory, the transfer rate between FPGA and off-chip memory affects the overall performance directly. The off-chip memory type and the width of the connected data bus are factors that determine the theoretical transfer rate. The FPGA acceleration cards employed in this research use DDR3 memory and the *HARP* platform uses DDR4 memory. Regarding the bit-width of the data bus, the *S5* card has two memory banks and connects each memory bank with a 64-bit data bus, which has 128-bit data bus in total. Regarding the *A10* card, each memory bank is connected with a 72-bit data bus, and the sum of two memory banks is 144. Hence, under the same operation frequency, the data transfer rate of *A10* is higher than that of *S5*.

The off-chip memory size affects the performance especially when multiple buffering is adopted. Take the triple buffering (in Figure 7) as an example, if the off-chip memory size is not large enough to hold three FOPs but will hold two FOPs, the implementation is restricted to double buffering. In this case, the execution latency for a new input array might be increased to  $t_{FDAS} - \max(t_{FT}, t_{FOP}, t_{HM})$ , which is larger than  $t_{FDAS}/2$ , assuming that  $\max(t_{FT}, t_{FOP}, t_{HM}) \leq t_{FDAS}/2$  (the case for triple buffering).

## Data Transfer Bus

The PCIe bus is the main connection between the host processor and FPGA devices. The transfer rate affects the performance especially when the data has to be transferred between the host and the device during processing. It is determined by the generation of the PCIe bus and the number of lanes connected to the FPGA devices. For example, PCIe Gen3.0 (used in the *A10* board) provides  $8.0\text{GTtransfers/s}$  per lane, while the latest Gen4.0 provides  $16.0\text{GTtransfers/s}$  per lane. The number of lanes can vary between 1 and 16 but is usually either 8 (used in the *S5* and *A10* board) or 16 for FPGA acceleration cards.

Besides the PCIe bus, the Intel QuickPath Interconnect (QPI) is employed in *HARP*. It is a point-to-point interconnect released by Intel. The QPI can be operated at up to  $4.8\text{GHz}$  and the data transfer rate can be tens of  $\text{GBytes/s}$ .

## Performance Factors

The performance of the pipelined FDAS module is mainly influenced by three factors: 1) parallelisation factor for each sub-module, 2) maximum frequency of the kernels, and 3) the global memory bandwidth.

### Parallelisation Factor

The optimised kernels as discuss in Section 2 almost fully exploit the target devices (such as their logic resources and off-chip memory bandwidth) and some kernels completely exhaust one type of resource such as the TDFIR kernel on *S5* consumes all DSP blocks. To integrate several kernels on one FPGA device, the optimised kernels need to compromise each other, and the straight-forward solution is to reduce the parallelisation factors of the optimised kernel. This obviously leads to an increase of the execution latency of the individual kernels.

### Kernel Frequency

The high percentage of resource usage of a combined kernel makes it complex and hard to be implemented by the OpenCL compiler and synthesis tools. This affects the maximum kernel frequency at which it can run, which directly influences the performance.

### Off-chip Memory Bandwidth

In pipeline computing, two or three kernels are executed simultaneously (Figure 7). If the total needed off-chip memory bandwidth surpasses the theoretical off-chip memory bandwidth, these kernels might not perform as fast as when executed. In this case, the maximum execution latency  $\max(t_{FT}, t_{FOP}, t_{HM})$  is increased and the performance drops.

## 3.4. Host and Device

### Data Transfer Approaches

For FPGA-based OpenCL, there are mainly two types of data transfer approaches between host and accelerator (FPGA). 1) general buffer transfer and 2) shared virtual memory (SVM).

#### General Buffer Transfer

In an OpenCL host program, a buffer object (one-dimensional) can be transferred between the device off-chip memory (i.e., OpenCL global memory) and the host memory using the `clEnqueueReadBuffer` and `clEnqueueWriteBuffer` functions. For two- or three-dimensional buffer, the `clEnqueueReadImage` and `clEnqueueWriteImage` are employed. The transfer is realised via the PCIe bus and the rate depends on its specification, see above.

#### Shared Virtual Memory

Using shared virtual memory (SVM) is a technique to extend the (OpenCL) global memory region into the host memory region. It is supported by the OpenCL 2.0 specification, and the host processor and

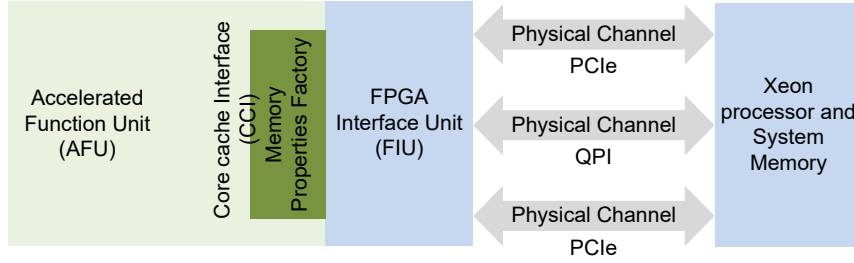


Figure 8. Intel Xeon Processor with FPGA IP

device(s) need a shared memory system. Since the *A10* and *S5* devices have no physical shared memory with the host and the SVM technique is not supported there. For the Intel Xeon processor platform with an integrated Arria 10 FPGA, referred to as Xeon+FPGA, the FPGA and processor are in the same package. An illustration of this is given in Figure 8. Inside the FPGA, the accelerated function unit (AFU) is available to be programmed by the developer, the other interfacing blocks are provided by Intel. The core cache interface (CCI) provides a base platform memory interface that exposes physical channels as a single, multiplexed read/write memory interface. The embedded FPGA is connected to the computer system memory (DDR4) through several physical channels such as PCIe and Intel QPI.

The memory properties factory (MPF) block is optional. When it is employed, it is instantiated as a CCI-to-CCI bridge, maintaining the same interface but adding new semantics. The main advantage of MPF is that it can translate the virtual address to a physical address and the FPGA and CPU can share pointers with each other.

SVM-based transfer is about 2x times faster than that of the general buffer-based transfer. By adding the FPGA to the chip-package, the physical design has to compromise with many additional constraints, and the performance of the processor part might not provide the same performance as the independent package processors of the same technology.

### *Tasks on the host*

The FPGA devices are employed as the accelerator, so naturally distributing and balancing tasks between the host and the device are investigated. Due to the usual performance penalty for transferring data between host and device, it is recommended to execute most or all tasks on the device. However, there are situations where data has to be transferred back to the host during processing.

- 1) The execution latency of a task on the host is significantly faster than that on the device.

Although FPGA devices perform better than the host in a wide range of applications, they still have a weak point in serial processing. If a task is arranged to be executed by the host, the data transfer rate between the host and devices becomes the main issue. Hence, when determining the performance advantage of the host processor or FPGAs, the inflicted data transfer delay needs to be considered in the analysis.

- 2) Data dependency of using multiple devices

This situation happens when multiple devices are employed in executing the same input array. The host can then become the master that needs to manage the dependences and communications between the sub-tasks and the devices. Of course, the ideal case in designing the FDAS module is to avoid transferring data between the host and devices while processing as much as possible.

### **3.5. Multiple Devices**

When employing more than one FPGA device for the acceleration, there are two obvious approaches: using 1) the same configuration (bitstream) file (single) or 2) different configuration files (multiple) for the

programming of the FPGA devices.

### *Single Configuration File*

#### Single Input Array

Multiple devices for a single input array can be necessary if  $t_{FDAS} > t_{limit}$ . Except for the MULTIPLEHP-R method in Section 2.2, the optimised harmonic-summing implementations on a single device take longer than the required time limit. When multiple devices ( $N_{devices}$ ) are employed, the harmonic-summing task can be split into  $N_{devices}$  independent parts and each FPGA device processes  $1/N_{devices}$  of the FOP. In this case, the ideal execution latency drops to  $\max(t_{FT}, t_{FOP}, t_{HM}/N_{devices})$ .

For the FT convolution module and FOP preparation module, each of the  $N_{devices}$  devices generates the full FOP, and it is unnecessary for a device to communicate with other devices while processing. Processing a single input array while all devices are configured with the same bitstream file, the same FOP is generated  $N_{devices}$  times.

#### Multiple Input Arrays

For multiple input arrays, the host sends  $N_{devices}$  different input array to  $N_{devices}$  FPGA devices and  $N_{devices}$  input arrays are processed in parallel. Compared with a single device, the ideal execution latency for multiple devices reduces to  $\max(t_{FT}, t_{FOP}, t_{HM})/N_{devices}$ ,

$$\frac{\max(t_{FT}, t_{FOP}, t_{HM})}{N_{devices}} \leq \max(t_{FT}, t_{FOP}, \frac{t_{HM}}{N_{devices}}).$$

Hence, the multiple input arrays approach has a theoretical advantage when  $t_{HM} = \max(t_{FT}, t_{FOP}, t_{HM})$ .

### *Multiple Configuration Files*

For some combinations, the FT convolution and harmonic-summing have to compromise with each other by reducing their parallelisation factors or scales. This leads to a decrease in performance for both parts. By using multiple devices, each device can be configured with one or two functions while taking full advantage of the device resources. In Figure 7, each stage can be assigned to a device and the number of buffering equals the number of devices. For example, when  $\max(t_{FT}, t_{FOP}, t_{HM}) < t_{FDAS}/2$ , three devices need to be installed and each device is configured with only one module.

The main problem with this method is the frequent communication between the host and the devices. The host needs to keep organizing data between different devices. This method requires a high transfer rate between the host and devices such as high generation PCIe and QPI.

### **3.6. A Case Study**

Before we systematically evaluate the pipeline design and the many combinations of the different sub-module kernels, let us have a closer look at the combination of the FDFIR+MULTIPLEHP-N kernels as a case study. The execution latency of one input array using three devices is depicted in Figure 9 (top). Three devices are configured with the same file and the harmonic-summing part of each device processes 1/3 of a half-FOP. The FDFIR filter is parallelised twice (i.e., two filters working in parallel), so the FT convolution kernel needs to be launched  $N_{FT-launch} = 21$  times (as there are 42 filters to be applied). Ignoring the FT convolution kernel launching overhead, the execution latency  $t_{FT}$  is  $\sum_{i=1}^{21} t'_{FT_i}$ . The FOP preparation kernel contains discard and transpose, and the harmonic summing kernel processes 1/3 of the overall task.

As can be seen in the basic execution latency (top),  $t_{HM} \geq \max(t_{FT}, t_{FOP})$  but smaller than  $t_{FDAS}/2$ . Based on the discussion in Section 3.3, we can infer the execution latency of multiple input arrays using triple buffering. Ideally, the execution latency of each part remains the same as that of executing one input array. The time cost for one new input array is  $t_{HM}$  in this example, Figure 9 (Middle).

However, the real execution latency of multiple input arrays takes much longer than the ideal case. The real result and details are given in Figure 9 (Bottom) as well. When the FOP preparation part is

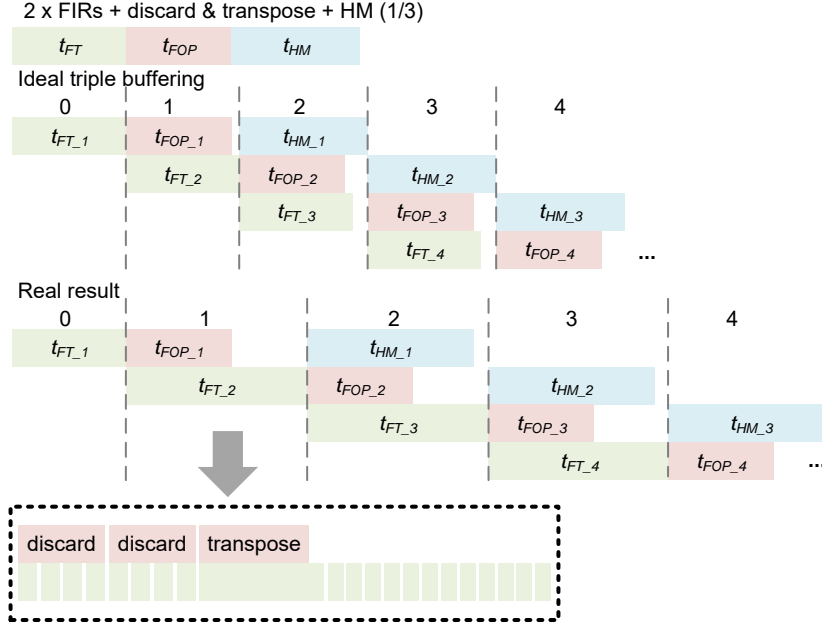


Figure 9. Ideal and real latencies of the kernels of the case study FDFIR+MULTIPLEHP-N

processing, the FT convolution part is severely affected, and the  $t_{HM}$  is increased as well. Because two FIR filters are working in parallel, the discard kernel is launched twice for two output groups. In the zoomed in part, during the discard processing, the FT convolution kernels are launched 8x times to process the next input array using 16 FIR filters, and the 9th FT convolution kernel is launched with the transpose kernel. The average value of  $t'_{FT_1}$  to  $t'_{FT_8}$  is larger than that of  $t'_{FT_{10}}$  to  $t'_{FT_{21}}$  and  $t'_{FT_9}$  is several times larger than others. The value of  $t'_{FT_9}$  is about the same as  $t_{discard} + \sum_{i=9}^{21} t'_{FT_i}/12$ .

The main reason for the stretch of  $t'_{FT_1}$  to  $t'_{FT_9}$  is the limited global memory bandwidth (GMB) of the FPGA device. The discard, transpose, and FT convolution kernels all depend heavily on the GMB. When two of them are processing at the same time, the needed GMB exceeds the device GMB. For the transpose kernel, it exhausts the device GMB while processing alone. When the transpose and FT convolution kernels are launched together, the FT convolution kernel is pended until the transpose kernel has been finished. When the three parts are processing in parallel, the value of  $t_{FT}$  will be larger than that of in the zoomed part in Figure 9. In real processing, the FT convolution becomes the dominant kernel and it determines the time delay until the next new input array can be processed (i.e., the pipeline period).

## 4. Experimental Evaluation

This section experimentally evaluates the design space of the FDAS module pipeline, by considering a large number of combinations of the optimised kernels of the sub-modules and their design parameters. The advantage of the multiple buffering technique is evaluated and multiple acceleration devices are employed to accelerate the FDAS module. The combinations are assessed according to their resource usage, execution latency, and energy dissipation and power consumption.

### 4.1. Resource Usage

High-end Arria 10 FPGAs (Nallatech 385A with Intel Arria 10 GX1150, in Table 2) are employed for the experiments. All combinations are implemented using Intel FPGA-based OpenCL, and all combined FDAS kernels are compiled using AOCL version 16.0.0.222.

For the FT convolution module, the OLA-TD and OLS-FD methods, in Section 2.1, are used. The OLA- $N_{paral}$  kernel, which parallelises  $N_{paral}$  complex SPF multiplications, and the AOLS- $N_{OLS-FT}$ , which

split the input array into a group of chunks whose each length is  $N_{OLS-FT}$ , are employed to combine with harmonic-summing modules. Taking the OLA-128 kernel as an example, it has to be launched four times to implement a 421-tap FIR filter, and its execution latency is the same as would be for a 512-tap FIR filter, as 91 taps are unused (set to zero).

For the harmonic summing modules, the SINGLEHP- $(S, R, 8)$  kernel is selected for the SINGLEHP method and the Naïve-MULTIPLEHP, MULTIPLEHP-N-(1), and MULTIPLEHP-R-(16, 4) are chosen for the MULTIPLEHP method. The parallelisation factors of the harmonic-summing module are the largest values that can be compiled successfully by the AOC when combining with the FT convolution module. The MULTIPLEHP-H method is based on the Naïve-MULTIPLEHP method and the best-performing implementation, which is MULTIPLEHP-H- $(5 \times 2^{13})$ , cannot be combined with other kernels as it exhausts the available FPGA resources. When the  $N_{MultipleHP-H-preld}$  is decreased to reduce resources, it performs worse than the Naïve-MULTIPLEHP kernel, so it is not considered in this research.

In summary, for the two types of FT convolution and the four types of the harmonic-summing, there are a total of eight FDAS combinations, listed in detail in Table 5. The table also provides resource usage and achievable frequencies of these combinations. Because each of the FT convolution and harmonic-summing parts contains at least one kernel, there are two or more independent kernels in the FDAS module. Each kernel in the FDAS module is compiled as an independent kernel. To arrange multiple independent kernels in a target FPGA, the compiler has to add more restrictions than compiling a single kernel. Although some successfully compiled kernels use less than half of the device resources, the parallelisation factors still cannot be increased as the compilation then fails. For each of the combinations in Table 5, several parallelisation factors are tested, and the combination with the fastest execution latency is recorded. Taking combination FDFIR+MULTIPLEHP-R as an example, AOLS-1024, AOLS-2048, and AOLS-4096 are combined with MULTIPLEHP-R-(16, 4), MULTIPLEHP-R-(16, 8), MULTIPLEHP-R-(64, 4), and MULTIPLEHP-R-(64, 8), which are 12 combinations in total. Among these 12 combinations, only three combinations can be successfully compiled. Of these three combinations, AOLS-2048+MULTIPLEHP-R-(16, 4) provides better performance than the other successfully compiled combinations such as AOLS-1024+MULTIPLEHP-R-(16, 4), hence it is the one recorded in the table.

Table 5. Resource usage of the combined FDAS kernels

	FT Convolution module	FOP preparation module	Harmonic-summing module	Frequency (MHz)	Logic utilisations	DSP blocks	RAM blocks
TDFIR	OLA-128	–	Naïve-MULTIPLEHP	207.8	25%	44%	42%
	OLA-256	–	Naïve-MULTIPLEHP	207.1	32%	86%	64%
	OLA-128	transpose	MULTIPLEHP-N-(1)	159.1	37%	43%	56%
	OLA-128	transpose+reorder	MULTIPLEHP-R-(16, 4)	182.2	47%	46%	52%
	OLA-128	–	MULTIPLEHP-R-(16, 4)	171.9	37%	46%	40%
	OLA-128	–	SINGLEHP- $(S, R, 8)$	179.6	45%	44%	49%
FDFIR	AOLS-2048	discard+transpose	Naïve-MULTIPLEHP	178.4	41%	23%	78%
	AOLS-2048	discard+transpose	MULTIPLEHP-N-(1)	175	35%	12%	66%
	AOLS-2048	discard+transpose+reorder	MULTIPLEHP-R-(16, 4)	180	49%	15%	56%
	AOLS-2048	–	MULTIPLEHP-R-(16, 4)	185.2	35%	15%	42%
	AOLS-2048	discard	SINGLEHP- $(S, R, 8)$	196.5	37%	23%	70%

Among these combinations, the OLA-128+Naïve-MULTIPLEHP and OLA-128+SINGLEHP- $(S, R, 8)$  do not require the FOP preparation kernel. For combinations that contain the MULTIPLEHP-R-(16, 4) kernel, if the FOP preparation task is assigned to the host processor, the FOP preparation module does not need to be implemented in the FPGA. The resource usage and kernel frequency of independent and combined implementations of these four kernels are given in Table 6. As expected, the frequency of the combined kernel is lower than each of its element kernels. The DSP block usage is slightly larger than the sum of element kernels. The logic cell and RAM blocks utilisations of a combined kernel are larger than that of each element kernel, however, smaller than the sum of all element kernels. The reason is that the default BSP package (i.e. interfacing IP blocks) costs logic cells and RAM blocks but is not using any DSP blocks



Table 6. Resource usage and kernel frequency of independent and combined implementations

Kernels	Frequency ( $HMz$ )			Logic utilization			DSP blocks			RAM blocks		
	FT	HM	Comb.	FT	HM	Comb.	FT	HM	Comb.	FT	HM	Comb.
OLA-128 + Naïve-MULTIPLEHP	267.4	227.06	207.9	21%	17%	25%	42%	<1%	44%	27%	27%	42%
OLA-128 + SINGLEHP-( $S, R, 8$ )	267.4	206.1	179.66	21%	42%	45%	42%	<1%	44%	27%	28%	49%
OLA-128 + MULTIPLEHP-R-(16, 4)	267.4	196.9	171.9	21%	30%	37%	42%	3%	46%	27%	37%	40%
AOLS-2048+ MULTIPLEHP-R-(16, 4)	252.3	196.9	185.2	16%	30%	35%	11%	3%	15%	32%	37%	42%

and is incurred only once, independent of the number of instantiated kernels.

#### 4.2. Latency Evaluation

We experimentally evaluated all the combinations of Table 5 and their execution latencies are given in Table 4.2. Only the single configuration file approach of Section 3.5 is employed in this section. The recorded values are the execution latencies of processing one input array ( $2^{21}$  complex SPF points) while applying 42 FIR filters (half of the FOP). Both serial processing and processing using the multiple buffering technique were evaluated. For multiple devices, only the multiple buffering-based processing approach is tested. The major positive observation from the results in Table 4.2 is that by applying the multiple buffering technique, the same kernel combination can achieve up to 2x speedup over non-multiple buffering based processing.

Except for the OLA-256+Naïve-MULTIPLEHP combination, all combinations that contain the OLA-TD method apply the OLA-128 kernel. The value 128 is the largest number of power of two that can be implemented within the combination. For the combination that contains the MULTIPLEHP-R method, the FOP preparation module is evaluated by executing on both host processor or FPGA device(s).

For combination AOLS+Naïve-MULTIPLEHP and combination AOLS+MULTIPLEHP-N, the  $t_{HM}$  is larger than  $\frac{1}{2}t_{FDAS}$ , so the single configuration file with single input array approach (in Section 3.5) is applied to split the harmonic-summing task evenly for multiple devices,  $\times 3$  in this research, see the last two rows of Table 4.2. For the configuration parameters of harmonic-summing kernels, the applied values are the largest that can be successfully compiled by AOC for the A10 FPGA. For the remaining combinations on three devices, they all process multiple input arrays in parallel.

Except for the FDFIR+MULTIPLEHP-R combination, the FDFIR-based combinations perform better than these TDFIR-based combinations. For combinations that contain the OLA-128 kernel, the execution latencies of the FT convolution part are all around 2s, which makes them noncompetitive with FDFIR-based combinations.

Regarding the FDFIR+MULTIPLEHP-R combination, even though the MULTIPLEHP-R method is the fastest among the proposed harmonic-summing methods, the FOP preparation part is inefficient and the FPGA-based implementation is slower than using the host processor. It takes 0.6s on the host processor and over 8s on an A10 device, which is over 12x times slower. For the FPGA-based implementation, the reorder part in the FOP preparation kernel has to leave enough resources for the main operations and it cannot be parallelised with a large parallelisation factor. This makes the execution latency of the FOP preparation part grow up to 8.4s. If the FOP preparation task is moved to the host processor, it can process one input array at a time using all threads, and the pipeline computing on multiple devices becomes impossible. By considering the FOP reordering, the advantage of the MULTIPLEHP-R method in low execution latency disappears.

#### Xeon+FPGA (HARP) and GPUs

The Intel HARP (Xeon+FPGA) platform, as introduced in Section 2, supports SVM-based data transfer and it is especially interesting to evaluate the combinations that require reordering on it. We evaluated the

Table 7. Execution latency of combined kernels on A10 cards

	FT Convolution module	FOP preparation module	Harmonic-summing module	No multiple buffering (ms)	Multiple buffering type	Pipeline period (ms)	Multiple devices $\times 3$ (ms)
TDFIR	OLA-128	–	Naïve-MULTIPLEHP	2,121	Double	1,698	568
	OLA-256	–	Naïve-MULTIPLEHP	1,278	Double	854	286
	OLA-128	transpose	MULTIPLEHP-N-(1)	2,916	Double	2,219	742
	OLA-128	transpose+reorder	MULTIPLEHP-R-(16, 4)	3,917	Double	1,935	647
	OLA-128	transpose+reorder (in host)	MULTIPLEHP-R-(16, 4)	2,727	Double	2,052	686
	OLA-128	–	SINGLEHP-( $S, R, 8$ )	2,662	Double	1,966	657
FDFIR	AOLS-2048	discard+transpose	Naïve-MULTIPLEHP	856	Double	570	190
	AOLS-2048	discard+transpose	MULTIPLEHP-N-(1)	976	Double	661	224
	AOLS-2048	discard+transpose+reorder	MULTIPLEHP-R-(16, 4)	8,780	Double	6,630	2,219
	AOLS-2048	discard+transpose+reorder (in host)	MULTIPLEHP-R-(16, 4)	972	Double	633	–
	AOLS-2048	discard	SINGLEHP-( $S, R, 8$ )	786	Double	682	237
	AOLS-2048	discard+transpose	$\frac{1}{3}$ Naïve-MULTIPLEHP	$523 \times 3$	Triple	$307 \times 3$	307
	AOLS-2048	discard+transpose	$\frac{1}{3}$ MULTIPLEHP-N-(1)	$587 \times 3$	Triple	$334 \times 3$	334

Table 8. Comparison of AOLS-2048+MULTIPLEHP-R-(16, 4) on HARP and I7 + A10 device

Platform	SVM transfer	Kernel frequency (MHz)	$t_{FT}$ (ms)	$t_{FOP}$ (ms)	$t_{HM}$ (ms)	$t_{FDAS}$ (ms)
HARP	Yes	225.0	347	560	122	1,029
I7 + A10	No	185.2	190	633	149	972

FDFIR+MULTIPLEHP-R combination (AOLS-2048+MULTIPLEHP-R-(16, 4)), and the results are given in Table 8. The same kernel can achieve higher kernel frequency on HARP than on the I7 + A10 system. While the execution latency of each FIR filter of the FT convolution module on HARP is shorter than on I7 + A10, the kernel launching overhead on HARP is higher, which makes the total execution latency of 42 FIR filters longer than that on I7 + A10. The main reason is that the host processor part of the HARP performs worse than I7. Regarding the FOP preparation module, which is processed on the host processor, the SVM transfer on HARP is about 1.7x times faster than the general transfer on I7 + A10. However, the performance of the host Xeon processor is over 1.6x times worse than that of the independent I7. This weakens the advantage of SVM-based implementation over the general transfer based implementation. It can be seen that the overall  $t_{FDAS}$  on the HARP platform is 6% lower than that on the I7 + A10.

Regarding the R7 GPU, since the single work-item kernels such as candidate detection and FOP preparation are efficient for GPUs, we only compare the combinations that consists of NDRange kernels to not distort the result in favour of the FPGAs. The details of the execution latencies of the GPU-based combinations are given in Table 9. The parallelisation factors are for the FPGA-based kernels and some of them do not work for GPU-based kernels. Though R7 supports running multiple kernels currently, the large number of work-groups of FT convolution kernels and harmonic-summing kernels make it fail to execute multiple kernels concurrently. It can be seen that the pipeline period of a single A10 is over 1.35x times slower than that of R7, however, three A10 cards provide better performance than R7. Also, remember that the R7 implementation does less work as candidate detection is not included.

Table 9. Comparison of NDRange kernels based combinations between  $A10$  and  $R7$ 

FT Convolution module	FOP preparation module	Harmonic-summing module	$t_{FT}$ (ms)	$t_{HM}$ (ms)	$t_{FDAS}$ (ms)	Speedup of $A10 \times 3$ over $R7 \times 1$
Naïve-TDFIR	–	Naïve-MULTIPLEHP	909	36	945	3.33
Naïve-TDFIR	–	SINGLEHP	909	20	929	1.41
AOLS-2048	(in the host)	MULTIPLEHP-R (no CD)	67	20	720	1.05

Table 10. Execution latencies of combinations with reduced  $N_{tap}$  using multiple buffering on three  $A10$  devices (ms)

$N_{tap}$	OLA-128+	OLA-128+	OLA-128+
	Naïve-MULTIPLEHP	MULTIPLEHP-N-(1)	SINGLEHP-( $S, R, 8$ )
421	568	742	657
256	283	370	328
128	142	226	235

### Less Filter Coefficients

Among the TDFIR-based combinations, OLA-256+Naïve-MULTIPLEHP is the fastest that is comparable with FDFIR-based combinations. If the average FIR length  $N_{tap}$  can be reduced, the performance of the TDFIR-based combinations become comparable with those of the FDFIR-based combinations. The execution performance of combinations with reduced  $N_{tap}$  is given in Table 10. Since the experiments so far showed that  $t_{FT}$  is dominating in the FDAS module for the TDFIR-based combinations, the decrease of  $N_{tap}$  directly leads to a reduced execution latency. Still, the  $t_{FT}$  of a TDFIR-based combination, after reducing  $N_{tap}$ , might be still be longer than that of FDFIR-based combinations. However, the sum of  $t_{FT} + t_{discard} + t_{transpose}$  for the FDFIR-based combination can be larger than the  $t_{FT}$  of the TDFIR-based combination.

### 4.3. Energy Dissipation and Power Consumption

In this section, we measure the power consumption and energy dissipation of the kernels on the  $A10$  cards. Since we have no physical access to the Intel Xeon+FPGA platform, we were not able to measure those metrics on that platform. Regarding the  $A10$  device, we measure the overall system power consumption in idle status  $P_{idle}$ , including FPGA device(s), and the running power  $P_{running}$  when the system is executing kernels on FPGA device(s). The real power consumption can be achieved by calculating the difference of  $P_{running}$  and  $P_{idle}$ . When an  $A10$  card is installed in the host, it costs about  $20W$  without launching any kernels. In this case, if the kernel is launched on a single FPGA, only one FPGA device is installed. For kernels running on three devices, three FPGA acceleration cards are installed. To make sure the measured  $P_{running}$  is stable, each combination is launched hundreds of times using a loop, which takes longer than one minute. The power consumption is measured using a plug-in power meter (Ego smart socket ESS-AU). When a device is configured with a new bitstream file, the  $P_{idle}$  might be changed slightly. To remove this interference factor, the power consumption of each combination is measured by 1) first shutting down the host for a minute to cool down the host and device(s), 2) boot the system, and 3) execute the kernel directly.

The power consumption and energy dissipation of different types of combinations on a single  $A10$  device are given in Table 11. The overall energy dissipation ( $P_{running} \times t_{MB}$ ) and absolute energy ( $(P_{running} - P_{idle}) \times t_{MB}$ ) dissipation are calculated based on  $P_{idle}$ ,  $P_{running}$ , and kernel execution latencies for one input array, where  $t_{MB}$  is the latency using the multiple buffering technique in Table 4.2 (using 42 FIR filters). Based on the number of installed devices the power consumption in idle status are  $P_{idle-FPGA \times 1} = 49W$  and  $P_{idle-FPGA \times 3} = 89W$ .

Table 11. Power consumption and energy dissipation of a single A10 device in executing the combined FDAS module

FDAS module Combinations	Pipeline computing	$P_{running}$ ( $W$ )	Overall energy ( $J$ )	Absolute energy ( $J$ )
FDFIR+MULTIPLEHP-R (FOP preparation in host)	No	66	180.2	46.4
FDFIR+MULTIPLEHP-R	No	59	519.2	88
FDFIR+Naïve-MULTIPLEHP	No	59	50.6	8.6
	Yes	60	30.6	6.3
FDFIR+MULTIPLEHP-N	No	60	58.6	10.7
	Yes	63	35.9	8
FDFIR+SINGLEHP	No	62	48.7	10.2
	Yes	64	43.5	10.2
TDFIR+SINGLEHP	No	60	159.7	29.3
	Yes	69	135.7	39.3
TDFIR+Naïve-MULTIPLEHP	No	57	120.8	17.0
	Yes	59	100.2	17.0
TDFIR+MULTIPLEHP-N	No	57	166.2	23.3
	Yes	59	130.9	22.2

The first observation is that the power consumption  $P_{running}$  does only vary between  $57W$  and  $69W$ , whereas the energy dissipation varies significantly more, which is of course due to the large difference in execution latencies (see Table 4.2). For the same combination, the overall energy dissipation by applying pipeline computing is lower than that without pipeline computing. Regarding the absolute energy dissipation, applying pipeline computing costs less energy for most of the combinations. For the TDFIR+SINGLEHP and TDFIR+Naïve-MULTIPLEHP combinations, the absolute energy dissipation of the pipeline computing based implementations are about the same as those of without pipeline computing. The reason is that the longest part of these combinations, which is  $max(t_{FT}, t_{FOP}, t_{HM})$ , takes a high proportion in the overall execution latency, hence the pipeline is not balanced enough to provide more benefit. FDFIR+SINGLEHP is the only combination that consumes more energy using pipeline computing. The main reason is that the ratio of  $t_{FT}/t_{FDAS}$  is over 75%, making the execution latency for a single input array close to the pipeline period, in other words, the pipelining is not efficient. In addition, the power consumption of pipeline computing is larger than that without pipeline computing, likely due to the need of additional buffers and the implicit communications and the fact that more processing is happening at the same time.

When three A10 are installed to accelerate the FDAS module, the  $P_{running}$  is about 2x times higher than those using the single A10 device, which is given in Table 12. The power consumption of the FDFIR+SINGLEHP combination is the highest among these implementations, however, the power consumption for three A10 cards is only  $104W$  ( $133W - 29W$ ), where  $P_{idle-noFPGA}$  is  $29W$ . It can be found that it is smaller than that of a single mid-range GPU device, not to mention high-end GPU platforms, which can cost up to  $300W$  per device. For the TDFIR+SINGLEHP combination on GPU (in Figure 9), the power consumption for one R7 card is  $97W$ , which is larger than the value in Table 12, which is  $88W$  ( $117W - 29W$ ).

By installing three devices, the overall energy dissipation of processing one input array drops when compared with single device-based processing. However, the absolute energy dissipations for FDFIR-based combinations are all increased to some degree (ratio is given in brackets). For the TDFIR-based combinations, the absolute energy dissipations are all decreased. For the FDFIR+Naïve-MULTIPLEHP combination, the implementation that processes one input array on three devices (each device processes 1/3 of half FOP) costs more energy than the implementation that processes three input arrays on three devices. Although

Table 12. Power consumption and energy dissipation of three  $A10$  devices in executing the FDAS module combinations using pipeline computing; energy ratios of using  $3 \times A10$  over  $1 \times A10$  are given in ( $\times*$ )

FDAS module Combinations	$P_{running}$ (W)	Overall energy (J)	Absolute energy (J)
FDFIR+SINGLEHP	133	30.3 ( $\times 1.4$ )	10.4 ( $\times 1$ )
FDFIR+Naïve-MULTIPLEHP	128	24.3 ( $\times 1.26$ )	7.4 ( $\times 0.85$ )
FDFIR+Naïve-MULTIPLEHP (1/3 of FOP)	126	38.7	11.4
FDFIR+MULTIPLEHP-N	123	27.6 ( $\times 1.3$ )	8.7 ( $\times 0.92$ )
TDFIR+SINGLEHP	117	76.8 ( $\times 1.77$ )	18.4 ( $\times 2.13$ )
TDFIR+Naïve-MULTIPLEHP	108	61.3 ( $\times 1.63$ )	10.8 ( $\times 1.57$ )
TDFIR+MULTIPLEHP-N	111	82.1 ( $\times 1.6$ )	16.3 ( $\times 1.36$ )

Table 13. Power consumption and energy dissipation of three  $A10$  devices in executing the FDAS module combinations using pipeline computing with reduced  $N_{tap}$  ( $N_{tap} = 128$ ); energy ratios of  $N_{tap} = 421$  over  $N_{tap} = 128$  are given in ( $\times*$ )

FDAS module Combinations	$P_{running}$ (W)	Overall energy (J)	Absolute energy (J)
TDFIR+SINGLEHP	119	27.965 ( $\times 2.7$ )	7.11 ( $\times 2.6$ )
TDFIR+Naïve-MULTIPLEHP	114	25.76 ( $\times 3.2$ )	5.65 ( $\times 2.9$ )
TDFIR+MULTIPLEHP-N	110	15.62 ( $\times 3.9$ )	2.982 ( $\times 3.6$ )

the processing one input array on three devices needs less power, the same FT convolution and FOP preparation tasks are redundantly executed three times to avoid communication. Among these combinations, the absolute costs of FDFIR+Naïve-MULTIPLEHP on the single device and three devices are both the smallest, so is the execution latency in Table 4.2.

Regarding the reduction of the average tap number  $N_{tap}$ , when  $N_{tap}$  is reduced from 421 to 128, the power consumption and energy dissipation of TDFIR-based combinations are decreased, and the overall energy consumption is up to 3.9x times less than that of the original implementation, which is shown in Table 13.

## 5. Conclusions

In paper we have investigated the combination of two well-optimised pulsar search modules: the FT convolution module and the harmonic-summing module. We explored the design space of the FDAS module combinations with different conditions and parallelisation factors using OpenCL. An FOP preparation module that transforms the FOP based on the demand of the two neighbouring modules was added to connect them. We also investigated multiple buffering strategies and assigning the tasks to multiple devices. As expected, after combining the well-optimised kernels, the frequency of the combined kernel was slower than any of its element kernels. The evaluation showed that the method with the best independent individual performance might not provide good performance when combined with other modules. Applying the multiple buffering technique, the combination kernel gains up to 2x times processing speedup. Among the evaluated combinations, the FDFIR+Naïve-MULTIPLEHP performed best and it needed less power and cost less energy than any other investigated combination. Most of the TDFIR-based combinations perform worse than the FDFIR-based combinations. When the average length of the FIR filters can be reduced,

the TDFIR-based combinations showed a high potential in achieving higher performance while costing less energy.

## Acknowledgment

The authors acknowledge discussions with the TDT, a collaboration between Manchester and Oxford Universities, and MPIFR Bonn and the work benefitted from their collaboration. We sincerely thank Intel for the donation of development tools and hardware access, especially access of the HARP systems.

## References

- Jim Costabile. Maxcompiler white paper, 2011.
- Tomasz S Czajkowski, Utku Aydonat, Dmitry Denisenko, John Freeman, Michael Kinsner, David Neto, Jason Wong, Peter Yiannacouras, and Deshanand P Singh. From opencl to high-performance hardware on fpgas. In *Field Programmable Logic and Applications (FPL), 2012 22nd International Conference on*, pages 531–534. IEEE, 2012.
- Peter E Dewdney, Peter J Hall, Richard T Schilizzi, and T Joseph LW Lazio. The square kilometre array. *Proceedings of the IEEE*, 97(8):1482–1496, 2009.
- Mario Garrido, Jesús Grajal, MA Sanchez, and Oscar Gustafsson. Pipelined radix-2k feedforward fft architectures. *IEEE Transactions on Very Large Scale Integration (VLSI) Systems*, 21(1):23–32, 2013.
- S Jouteux, R Ramachandran, BW Stappers, PG Jonker, and M Van Der Klis. Searching for pulsars in close circular binary systems. *Astronomy & Astrophysics*, 384(2):532–544, 2002.
- Karas Pavel and Svoboda David. Algorithms for efficient computation of convolution. In *Design and Architectures for Digital Signal Processing*. InTech, 2013.
- Scott M Ransom. Fast search techniques for high energy pulsars. *arXiv preprint astro-ph/0112006*, 2001.
- Scott M Ransom, Stephen S Eikenberry, and John Middleditch. Fourier techniques for very long astrophysical time-series analysis. *The Astronomical Journal*, 124(3):1788, 2002.
- Steven W Smith et al. The scientist and engineer’s guide to digital signal processing. 1997.
- Haomiao Wang, Prabu Thiagaraj, and Oliver Sinnen. Fpga-based acceleration of ft convolution for pulsar search using opencl. *arXiv preprint arXiv:1805.12280*, 2018.
- Haomiao Wang, Prabu Thiagaraj, and Oliver Sinnen. Harmonic-summing module of ska on fpga—optimising the irregular memory accesses. *arXiv preprint arXiv:1805.12258*, 2018.
- Haomiao Wang, Ming Zhang, Prabu Thiagaraj, and Oliver Sinnen. Fpga-based acceleration of fdas module using opencl. In *Field-Programmable Technology (FPT), 2016 International Conference on*, pages 53–60. IEEE, 2016.
- Markus Weinhardt and Wayne Luk. Memory access optimization and ram inference for pipeline vectorization. In *FPL*, pages 61–70. Springer, 1999.